

Auxetic Foam for Snow-Sport Safety Devices

Tom Allen, Olly Duncan, Leon Foster, Terry Senior, Davide Zampieri, Victor Edeh, and Andrew Alderson

Abstract Skiing and snowboarding are popular snow-sports with inherent risk of injury. There is potential to reduce the prevalence of injuries by improving and implementing snow-sport safety devices with the application of advanced materials. This chapter investigates the application of auxetic foam to snow-sport safety devices. Composite pads—consisting of foam covered with a semi-rigid shell—were investigated as a simple model of body armour and a large 70 × 355 × 355 mm auxetic foam sample was fabricated as an example crash barrier. The thermo-mechanical conversion process was applied to convert open-cell polyurethane foam to auxetic foam. The composite pad with auxetic foam absorbed around three times more energy than the conventional equivalent under quasi-static compression with a concentrated load, indicating potential for body armour applications. An adapted thermo-mechanical process—utilising through-thickness rods to control in-plane compression—was applied to fabricate the large sample with relatively consistent properties throughout, indicating further potential for fabrication of a full size auxetic crash barrier. Further work will create full size prototypes of snow-sport safety devices with comparative testing against current products.

Keywords Skiing • Padding • Impact protection • Snowboarding • Material

1 Introduction

Alpine skiing and snowboarding are popular Winter Olympic Sports. Worldwide participation numbers are hard to predict, but there are an estimated 115 to 200 million skiers [1, 2] and 10 to 15 million snowboarders [3–5]. Despite the popularity of snow-sports, there are inherent risks of injury, and even death. Snowboarders are at

T. Allen (✉)
Manchester Metropolitan University, Manchester, UK
e-mail: t.allen@mmu.ac.uk

O. Duncan • L. Foster • T. Senior • D. Zampieri • V. Edeh • A. Alderson
Sheffield Hallam University, Sheffield, UK
e-mail: A.Alderson@shu.ac.uk

greater risk of injury than skiers [6–8], with estimates ranging from 1 to 15 injuries per 1,000 riding days [9, 10]. The upper extremities are particularly at risk among snowboarders [7, 9, 11, 12], with wrist injuries common for beginners and children [7, 13–16].

Falls account for the most snow-sport injuries, contributing to 43 to 73% of injuries for skiers and 69 to 93% of injuries for snowboarders [17]. Experienced participants experience the greatest incidence of injuries when attempting jumps [18]. Devices are available for reducing injuries; these include crash barriers and personal protective equipment (PPE). Crash barriers are often large foam pads, designed to limit peak force in the event of a collision with a fixed object. Personal protective equipment includes helmets, wrist protectors and body armour such as back protectors.

Standards ensure certified snow-sport helmets limit peak force (e.g. EN1077 [19] and ASTM F2040 [20]) and resist penetration (e.g. EN1077), but they do not always provide for protection against concussion [12]. There are no snow-sport-specific standards for wrist protectors [16] or back protectors [21]. There is consensus that wrist protectors can prevent injuries by absorbing energy and limiting hyperextension, but it is unclear which designs offer the most protection [16]. Back protectors come in two primary forms, a hard shell with padding underneath offering greater resistance to penetration, and foam in isolation which absorbs more impact energy [21]. Snow-sport safety devices might be improved through design changes including the application of advanced materials which could allow reduced bulk, increased comfort and greater protection across a range of scenarios.

A number of studies present a case for applying auxetic foam to sport safety devices [e.g. 22–26], and there are patents for sportswear with auxetic components [27–29]. Auxetic foams are characterised by a negative Poisson's ratio; when compressed in one direction these materials contract in one or more perpendicular directions. This contraction and densification under the region of contact can lead to increased indentation resistance [30], which could be particularly beneficial to snow-sport safety devices. The indentation resistance (H) for an isotropic material is related to Poisson's ratio (ν) and Young's modulus (E),

$$H \propto \left[\frac{(1-\nu^2)}{E} \right]^{-x} \quad (1)$$

where x depends on the indenter shape [31]. For isotropic materials, the thermodynamically allowable upper and lower limits for Poisson's ratio are +0.5 and -1.0, respectively. Hence, for a given Young's modulus, indentation resistance will have a maximum finite value when Poisson's ratio equals +0.5 for conventional (positive Poisson's ratio) materials, whereas it increases towards infinity as Poisson's ratio tends towards -1.0 for auxetic materials.

1.1 Auxetic Foam

Despite the wealth of research into auxetic foam, work is needed to determine how best to fabricate and apply it to snow-sport safety devices. The general mechanism involves compression of conventional foam, followed by softening and then stiffening in the compressed state to give a re-entrant cell structure, as outlined in Lakes [32]. Heating to around the “softening temperature” is the common method of softening (“thermo-mechanical softening”) [e.g. 24, 32–35] although a chemical bath can also be used (“chemical–mechanical” or “mechanical–chemical–thermal softening”) [36, 37]. Increasing volumetric compression ratio (VCR—ratio of uncompressed to compressed volume), up to a limit of approximately five, generally enhances auxetic behaviour and lowers Poisson’s ratio [24, 33]. The conversion process can be applied to a range of materials [e.g. 34, 38], and highly anisotropic auxetic foam can be obtained by applying different amounts of compression in each direction during fabrication [39].

When applying the thermo-mechanical process, there is, as yet, no consensus regarding the best heating time and temperature combination to maximise auxetic behaviour. Differences may be due to variations in foam properties between studies, the VCR applied and the size of fabricated samples. Early exploratory studies produced small samples of auxetic foam [e.g. 32, 38], while recent work has produced larger samples as the research moves closer to commercial applications [23–25, 40, 41]. Producing large samples is challenging as the thermo-mechanical process can result in inhomogeneous auxetic foam due to non-uniform temperature and compression gradients present during fabrication [25, 33, 40, 42]. A reliable method of fabricating large volumes of auxetic foam is therefore required to facilitate production and testing for snow-sport safety applications, including monoliths for crash pads and sheets for body armour.

Auxetic behaviour is identified by confirmation of a negative Poisson’s ratio. Poisson’s ratio is often measured during low-speed stretching or compression, by tracking the position of markers on a sample followed by linear regression of lateral-strain vs. axial-strain data in the low axial-strain region [e.g. 25, 34]. Negative Poisson’s ratios have been measured for auxetic foams subject to high-speed compression [24, 43]. This is especially relevant to snow-sport safety devices, which are typically required to absorb energy through compression at relatively high speed. Work exploring snow-sport safety applications of auxetic foams should, therefore, involve testing at high strains and strain rates, for both crash pads and body armour.

Auxetic foams have higher resilience [24, 32] and absorb more energy [44] under compression compared to their conventional open-cell counterparts. Their stress–strain curves have an extended quasi-linear region and the foam densifies earlier as a result of lateral contraction [34]. This lateral contraction can cause auxetic foam to deform less in the direction of the applied load under impact [23] and reduce peak force in comparison to conventional open-cell foam [23, 24]. Auxetic foams have been shown to be particularly effective at limiting forces from concentrated impact loads when combined with a semi-rigid shell [24, 25], which should lend them well to padding in body armour.

2 Objective

Auxetic foams offer potential to improve snow-sport safety devices, such as body armour or crash pads. Work is required to determine how best these novel materials can be utilised. This work will explore applications for body armour, by examining the energy absorbed by a composite pad consisting of an auxetic foam sheet and semi-rigid shell subject to a load–unload cycle. The feasibility of producing auxetic foam crash pads will be explored by applying an adapted thermo-mechanical process to fabricate a large sized sample.

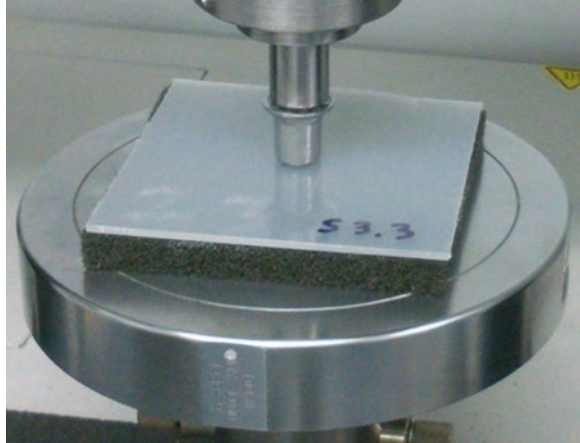
3 Methods

Open-cell polyurethane foam (R30RF and R60RF, supplied by Custom Foams) was converted to auxetic foam. The foam has a working temperature range of -40 to $+120$ °C (as specified by the supplier), indicating it is suitable for use in typical climate conditions for snow-sports. Foam of the same type has been used in previous work [e.g. 24, 26] and similar thermo-mechanical conversion processes were adopted here. Over-sized foam samples were compressed in a metal mould consisting of two U-shaped parts, with the internal faces lubricated with olive oil. The mould containing the compressed foam was placed in an oven at 180 °C for two heating phases followed by a 20 min annealing phase at 100 °C. The heating time was dependent on the size of the foam sample. Each sample was removed from the mould after each phase and gently stretched by hand to reduce adhesion of cell ribs. Following annealing the foam was left to cool to room temperature in the mould. Poisson's ratio was measured from quasi-static tests by filming pins in a sample while it was being stretched or compressed. The video footage was analysed later with a Matlab (Mathworks) script, which automatically tracked the positions of the pins to obtain true strain. Details of the methods for the body armour and crash pad examples are described below.

3.1 Body Armour

Composites pads—consisting of a $10 \times 90 \times 90$ mm or $20 \times 90 \times 90$ mm foam sample covered with a $4 \times 90 \times 90$ mm polypropylene (PP) sheet (Direct Plastics, PPH/PP-DWST-Homopolymer)—were investigated as a simple model of body armour. The larger pads had similar thickness to commercially available back protectors [21]. To help ensure uniform compression and temperature and the production of homogeneous samples, auxetic foam sheets were converted individually at the required thickness, rather than converting and then slicing a cube [26]. Foam (R30RF and R60RF) samples ($15 \times 143 \times 143$ mm and $30 \times 143 \times 143$ mm) were

Fig. 1 Compression test set-up displaying foam sample, PP shell and stud used to apply a concentrated load

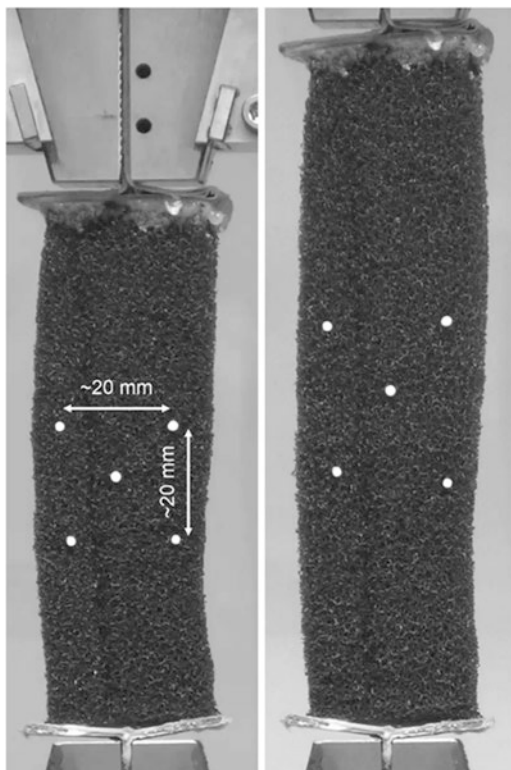


compressed to 70% of their original size along each dimension in a mould, resulting in a VCR of 3. The heating phases at 180 °C were 25 min long. After a week, a 5 mm wide strip was cut from each side of the foam cuboids to leave 10 × 90 × 90 mm or 20 × 90 × 90 mm samples. Thirteen samples were fabricated, six 10 mm thick and seven 20 mm thick. Two 10 × 90 × 90 mm and two 20 × 90 × 90 mm samples of unconverted foam (R60RF) were cut from a monolith for comparative testing.

Concentrated load compression testing (Instron 3369, fitted with a 50 kN load cell) was performed with a PP sheet placed unbonded on top of each sample. The pad rested on a flat plate and a load was applied to the centre of the upper face with a stud (Kipsta, aluminium football stud, 18 mm length) as shown in Fig. 1. Pilot testing confirmed the efficacy of the set-up for providing intermediate behaviour between compressing foam in isolation between two flat plates, and a stud and a flat plate. Following application of a small preload (approximately 1 N), the pad was compressed and unloaded in a cycle to 60% of the foam thickness (6 mm and 12 mm) at 3 mm/min. Energy absorbed was calculated as the difference between the area under the loading and unloading curve.

Chan and Evans [34] reported slightly lower Poisson's ratios for auxetic foam under tension in comparison to compression. In this work, Poisson's ratio was measured in tension to avoid issues with, (1) contact surface friction when compression testing thin sheets [24–26] and, (2) positioning and tracking pins in a small sample (cut from the sheet) under compression. After testing the pads, a sample of auxetic foam of each thickness and porosity was cut into three equal strips (resulting in six measuring 10 × 30 × 90 mm and six measuring 20 × 30 × 90 mm in total) and cardboard was glued to the ends so they could be gripped (Fig. 2). Each sample was stretched at 10 mm/min (strain rate of 0.002 s⁻¹) to 30% extension. Four pins in a 20 × 20 mm square in the face of the sample were filmed with a camera (JVC Everio Full HD resolution 1920 × 1080 pixels) and Poisson's ratio was obtained from linear regression of true lateral-strain vs. true axial-strain data up to 10% extension.

Fig. 2 Tensile test set-up displaying pins used to measure Poisson's ratio, (*Left*) no extension and (*Right*) maximum extension



3.2 Crash Pad

A $70 \times 355 \times 355$ mm auxetic foam sample was created by compressing a $96 \times 445 \times 445$ mm foam monolith into a mould with internal dimensions measuring $70 \times 355 \times 355$, to give a VCR of 2. Through-thickness compression was marginally higher to account for elongated cells in the rise direction. Following the methods of Duncan et al. [26], through-thickness metal rods were used to help fit the foam into the mould, control in-plane compression and draw heat through the porous material (Fig. 3).

The face of each half of the mould contained a grid of 36 holes, with a diameter of 3.5 mm and an equal spacing of 50 mm (Fig. 3a). An equal number of rods with a diameter of 3 mm were inserted through the thickness of the uncompressed foam with 61 mm spacing (Fig. 3b). The rods passed through the corresponding holes in the two halves of the mould as they came together, helping to draw the foam into place (Fig. 3c, d). The heating phases at 180°C were 35 min long, with the rods removed after the first and not returned. The dimensions of the sample were measured after cooling and then 7 days later to confirm the foam was stable and had not expanded.

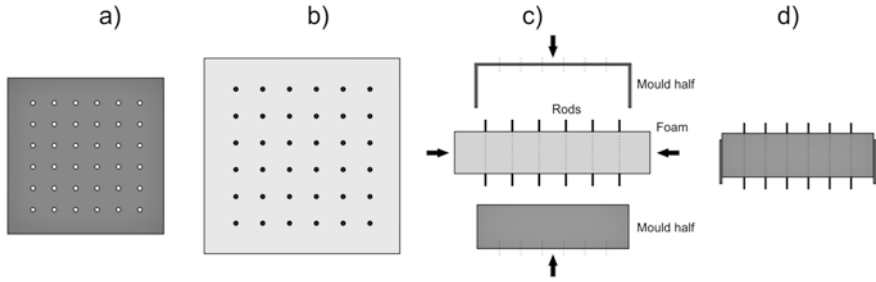


Fig. 3 Process used to fit the large foam sample into the mould, (a) top view of mould half with holes for rods, (b) top view of uncompressed foam with rods inserted, (c) illustration of foam compression into mould, and (d) side view of mould containing compressed foam with through-thickness rods

Three $50 \times 50 \times 70$ mm samples were cut from the converted foam with a band-saw, corresponding to the centre, corner and centre of an edge (Fig. 4). Each sample was compressed (Instron 3367, fitted with a 5 kN load cell) three times between two flat plates along the longest dimension (70 mm) to 50% strain at 10 mm/min (strain rate of 0.002 s^{-1}). Pins in the face of the sample were filmed with a camera (Sony Handycam HFR-CX410 operating at 25 Hz) to obtain true strain (Fig. 5) in both directions. Two pins approximately midway up the sample and around 30 mm apart were used for true lateral-strain and four pins arranged in a rectangle around the centre were used for true axial-strain. Poisson's ratio was obtained from linear regression of the true lateral-strain vs. true axial-strain data up to 50% compression.

Density measurements of the samples were used to examine local variations in VCR and images of the foam were obtained with an optical microscope (Leica S6D) to examine cell structure.

4 Results

4.1 Body Armour

Figure 6a show lateral-strain vs. axial-strain from a tensile test of auxetic foam. Averaged across all 12 samples, mean Poisson's ratio was -0.01 with a standard deviation of 0.13, suggesting marginally auxetic behaviour. Figure 6b, c shows example force–displacement curves for concentrated load compression tests of pads. The pads containing conventional foam exhibited an initial region of high stiffness, followed by a plateau region with evidence of densification towards maximum compression. In contrast, pads containing auxetic foam exhibited an extended region of quasi-linear stiffness up to approximately 50% compression of the foam, followed by a region of increasing stiffness. The shape of these loading curves are similar to those reported for quasi-static compression testing of conventional and auxetic foam between two flat plates [32, 44].

Fig. 4 (a) Large ($70 \times 355 \times 355$ mm) sample of converted foam with samples removed and (b) $50 \times 50 \times 70$ mm samples cut from large sample of converted foam

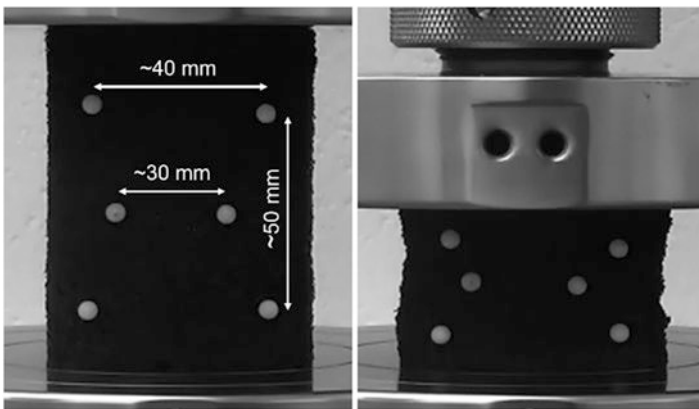
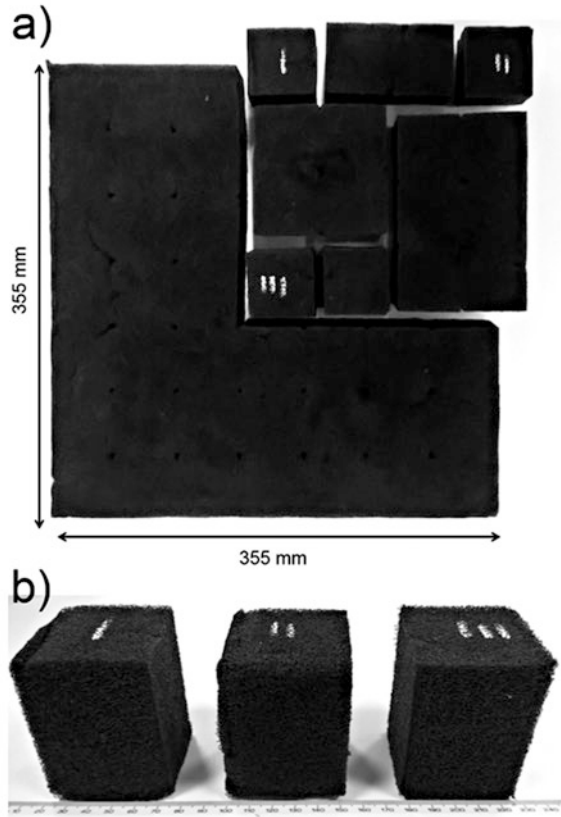


Fig. 5 Compression test set-up displaying pins used to measure Poisson's ratio, *Left*) No compression and *Right*) Maximum compression

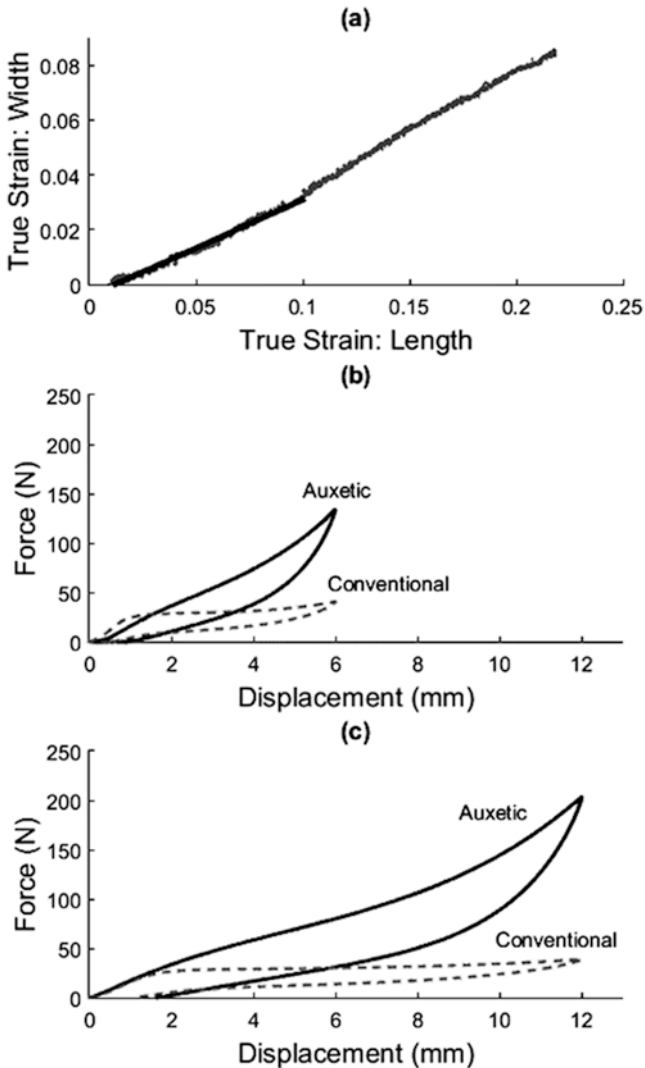


Fig. 6 (a) Strain–strain data for a tensile test on a 10 × 30 × 90 mm sample of R30RF auxetic foam, showing linear trend line used to obtain a Poisson’s ratio of -0.4 . Example force–displacement relationships for concentrated load quasi-static compression on composite pads consisting of an R60RF foam sheet and 4 mm thick polypropylene shell, (b) 10 mm thick foam and (c) 20 mm thick foam

Figure 7 summarises peak force and energy absorbed for the concentrated load compression tests on the pads. Peak force was approximately four times higher for the thin auxetic pads compared to their conventional counterparts and approximately five times higher for the thick auxetic pads than their conventional equivalents. For a given foam, the energy absorbed in the compression cycle increased with pad

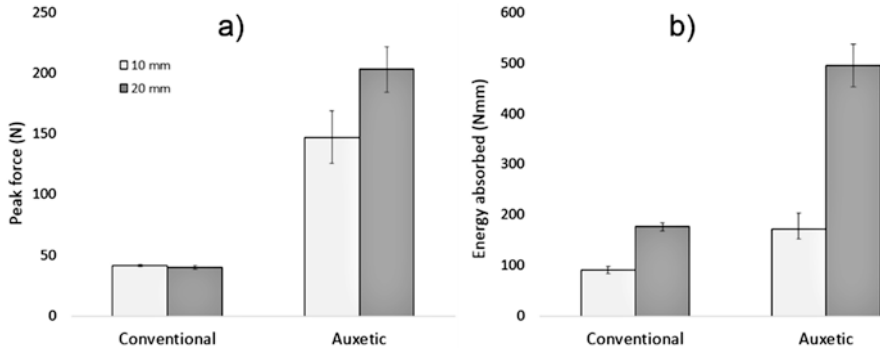


Fig. 7 Concentrated load compression testing results, (a) Peak force and (b) Energy absorbed. Error bars correspond to one standard deviation either side

thickness. The thinner pads with auxetic foam absorbed around twice as much energy as their unconverted counterparts, while the thicker auxetic pads absorbed approximately three times more energy than their conventional equivalents.

4.2 Crash Barrier

Figure 8a shows example compressive stress–strain curves for samples from the large foam conversion. The curves all show an extended quasi-linear region followed by progressive stiffening at approximately 30% compression, characteristic of auxetic foam [32, 35]. The corner sample was slightly stiffer above approximately 20% compression, with maximum stress ranging from 13 to 16 kPa in comparison to 11 to 13 kPa for the edge and centre samples. Figure 8b shows an example true lateral-strain vs. true axial-strain curve for the centre sample from the large foam conversion. Poisson’s ratio was -0.078 ± 0.014 (mean \pm standard deviation) for the corner sample, -0.013 ± 0.003 for the edge sample and -0.068 ± 0.010 for the centre sample, indicating marginally auxetic behaviour. Density measurements confirmed a VCR of approximately 2 for all samples. Figure 9 shows the conventional foam had a regular cell structure and all the converted foam samples had a re-entrant cell structure, characteristic of auxetic foam.

5 Discussion

Composite pads—consisting of a sheet of auxetic foam and a semi-rigid shell—absorbed approximately three times more energy than their conventional equivalent, under quasi-static compression with a concentrated load. Auxetic pads were also

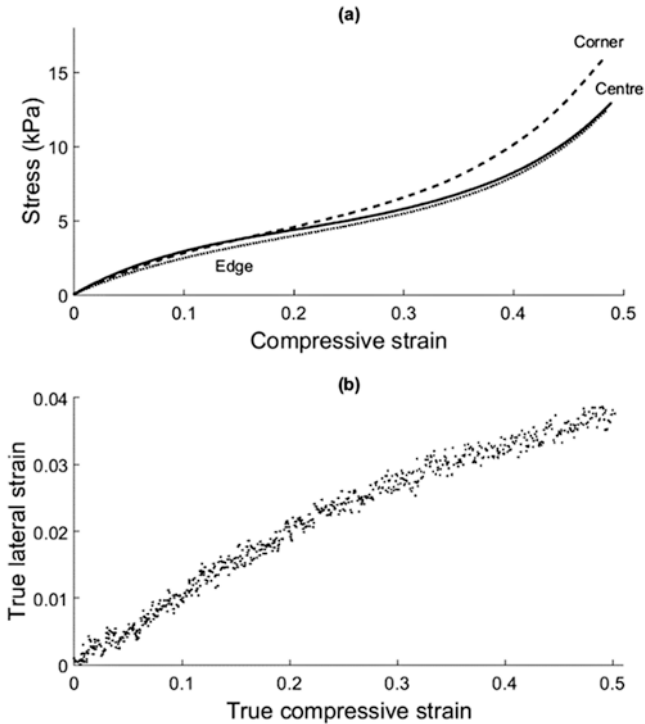


Fig. 8 (a) Example stress–strain relationship for quasi-static compression of $50 \times 50 \times 70$ mm samples cut from the $70 \times 355 \times 355$ mm sample of converted foam and (b) strain–strain relationship for the centre sample

stiffer with peak force approximately five times higher when compressed to 60% of the foam thickness, which will likely offer greater resistance to bottoming out under impact, as reported previously [24–26]. These results show further potential for auxetic foam as an energy-absorbing component in PPE for snow-sports, such as back or wrist protectors. Relatively low stiffness foam was used here and further work should aim to fabricate stiffer auxetic foam that is more representative of foam typically used in PPE.

A modified thermo-mechanical conversion process—utilising through-thickness rods to provide greater control over in-plane compression—was applied to produce a relatively large sample ($70 \times 355 \times 355$ mm) of auxetic foam as an example crash pad. Analysis of samples taken from different locations in the pad showed relatively consistent stress–strain curves, densities and Poisson’s ratios, with a re-entrant cell structure throughout, indicating the new process can produce large quasi-homogeneous monoliths of auxetic foam. The new process can now be applied to produce samples with different VCRs, as the amount of compression during fabrication can influence impact performance [24]. Despite the relatively large size of the

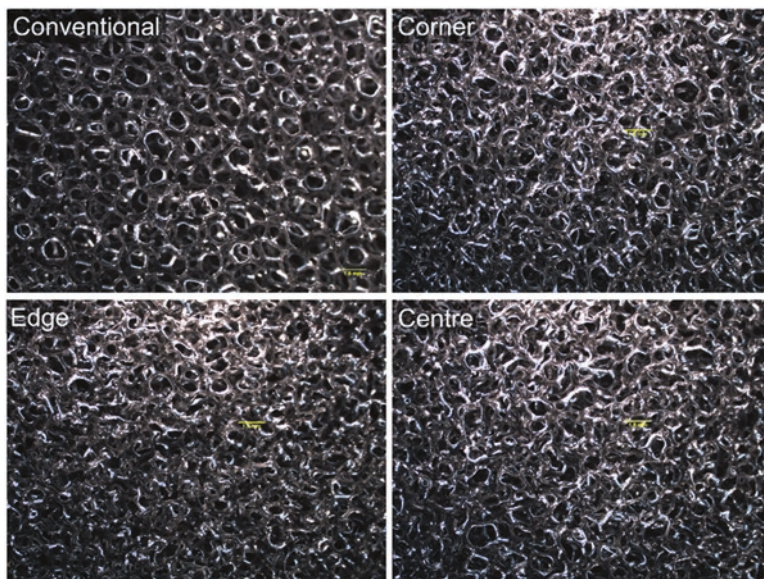


Fig. 9 Microscope images of cell structure for conventional foam and samples cut from the large conversion, (Top left) conventional foam, (Top right) Corner, (Bottom left) Edge, (Bottom right) Centre. The yellow scale line represents 1.5 mm

example auxetic pad in comparison to samples typically reported in the literature, it was smaller than a snow-sport safety crash barrier. Future work will, therefore, apply the new technique to produce a full size crash pad with comparative testing against current products.

Low temperature performance is important for snow-sport safety devices, and this needs careful consideration in further work investigating the application of auxetic foam. Different candidate foams should be investigated with a focus on identifying those with the most suitable working temperature range for snow-sports applications. EN1077 specifies snow-sports helmets to be acclimatised at both 20 °C and -25 °C prior to testing and a similar temperature range could be used as a starting point when characterising auxetic foam. Crash barriers will be repeatedly subject to extreme climate conditions on the mountain for extended periods of time, whereas body armour is typically worn underneath clothing where the minimum temperature should be higher. Future work should look towards identifying the most suitable candidate foams for specific applications.

The work presented here has shown further potential for auxetic foam to be applied to snow-sport safety devices. Future work will apply the new conversion process to produce larger sized samples, while tailoring mechanical properties of the auxetic foam to specific applications. Fabrication of prototypes and impact test-

ing for scenarios representative of snow-sport collisions is required. Impact testing of auxetic foam should be performed at temperatures typical of those where snow-sport is practised and the effect of repeated loading should be investigated.

References

1. Hunter RE (1999) Skiing injuries. *Am J Sports Med* 27(3):381–389
2. Vanat L (2014) International report on snow & mountain tourism. <http://www.vanat.ch/RM-world-report-2015.pdf>. Accessed 22 Dec 2015
3. Dann K (2011) Snowboarding. In: Engelhardt M, Dorr A (eds) *Sports orthopaedics*. Elsevier, Official Manual of GOTS, pp 637–645
4. Hasler RM, Berov S, Benneker L et al (2010) Are there risk factors for snowboard injuries? a case-control multicentre study of 559 snowboarders. *Br J Sports Med* 44(11):816–821
5. Kusche H, Gutsfeld P, Bühren V (2010) Snowboarden. *Sport Orthop Sport Traumatol* 26(3):178–181
6. Hagel BE, Goulet C, Platt RW et al (2004) Injuries among skiers and snowboarders in Quebec. *Epidemiology* 15(3):279–286
7. Russell K, Hagel B, Francescutti LH (2007) The effect of wrist guards on wrist and arm injuries among snowboarders: a systematic review. *Clin J Sport Med* 17(2):145–150
8. Sasaki K, Takagi M, Ida H et al (1999) Severity of upper limb injuries in snowboarding. *Arch Orthop Trauma Surg* 119(5–6):292–295
9. Russell K, Hagel B, Goulet C (2010) Snowboarding. In: Caine DJ, Harmer PA, Schiff MA (eds) *Epidemiology of injuries in olympic sports*, vol XVI. Blackwell Publishing, Oxford, pp 447–472
10. Machold W, Kwasny O, Gäler P et al (2000) Risk of injury through snowboarding. *J Trauma Acute Care Surg* 48(6):1109–1114
11. Kim S, Lee SK (2011) Snowboard wrist guards-use, efficacy, and design: a systematic review. *Bull NYU Hosp Jt Dis* 69(2):149–157
12. Brügger O, Bianchi G, Schulz D et al (2010) Snow-sport helmets: injury prevention, rate of wearers and recommendations. Berne: bfu-Swiss Council for Accident Prevention. EuroSafe Task Force Safety in Sports
13. Matsumoto K, Sumi H, Sumi Y et al (2004) Wrist fractures from snowboarding: a prospective study for 3 seasons from 1998 to 2001. *Clin J Sport Med* 14:64–71
14. Torjussen J, Bahr R (2005) Injuries among competitive snowboarders at the national elite level. *Am J Sports Med* 33(3):370–377
15. Dickson TJ (2009) Risk factors in snowboarder's wrist fractures. In: Senner V, Fastenbauer V, Bohm H (eds) *Proceedings of the 18th Congress of the International Society for Skiing Safety (ISSS)*. Technical University of Munich, Department of Sport Equipment and Materials, Garmisch-Partenkirchen, p 13
16. Michel FI, Schmitt KU, Greenwald RM et al (2013) White paper: functionality and efficacy of wrist protectors in snowboarding—towards a harmonized international standard. *Sports Eng* 16(4):197–210
17. Hagel B (2005) Skiing and snowboarding injuries. In: Caine DJ, Maffulli N (eds) *Epidemiology of pediatric sports injuries, individual sports*. Med sport sci, vol 48. Karger, Basel, pp 74–119
18. Hume PA, Lorimer AV, Griffiths PC et al (2015) Recreational snow-sports injury risk factors and countermeasures: a meta-analysis review and Haddon matrix evaluation. *Sports Med* 45(8):1–16
19. European Committee for Standardization (2007) Helmets for alpine skiers and snowboarders; EN 1077: 2007. EN 1077: 2007. European Committee for Standardization, Brussels

20. American Society for Testing and Materials (ASTM) (2002) ASTM F 2040-02: standard specification for helmets used for recreational snow sports. West Conshohocken
21. Schmitt KU, Liechti B, Michel FI et al (2010) Are current back protectors suitable to prevent spinal injury in recreational snowboarders? *Br J Sports Med* 44(11):822–826
22. Sanami M et al (2014) Auxetic materials for sports applications. In: James D, Choppin S, Allen T, Wheat J, Fleming P (eds) *The Engineering of Sport 10*, 10th Conference of the International Sports Engineering Association, Sheffield, July 2015, vol 72. *Procedia Engineering*, pp 453–458
23. Allen T et al (2015) Auxetic foams for sport safety applications. In: Subic A, Fuss FK, Alam F, Pang TY, Takla M (eds) *The Impact of Technology on Sport VI*. 7th Asia-Pacific Congress on Sports Technology, Barcelona, September 2015, vol 112. *Procedia Engineering*, pp 104–109
24. Allen T, Shepherd J, Hewage TAM et al (2015) Low-kinetic energy impact response of auxetic and conventional open-cell polyurethane foams. *Phys Status Solidi B* 252(7):1631–1639
25. Duncan O, Foster L, Senior T et al (2016) Quasi-static characterisation and impact testing of auxetic foam for sports safety applications. *Smart Mater Struct* 25(5):1–9
26. Duncan O, Foster L, Senior T, et al (2016) A comparison of novel and conventional fabrication methods for auxetic foams for sports safety applications. In: *The Engineering of Sport 11*. 11th Conference of the International Sports Engineering Association, Delft, July 2016, vol 147. *Procedia Engineering*, pp 384–389
27. Cross TM, Hoffer KW, Jones DP et al (2015) Auxetic structures and footwear with soles having auxetic structures. US patent 20,150,245,685, 3 Sep 2015
28. Bentham M, Alderson A, Alderson KL (2008) Garments having auxetic foam layers. US patent 7,455,567, 25 Nov 2008
29. Toronjo A (2013) Articles of apparel including auxetic materials. US Patent Application 13/838,827, filed 15 March 2013
30. Chan N, Evans KE (1998) Indentation resilience of conventional and auxetic foams. *J Cell Plast* 34(3):231–260
31. Evans KE, Alderson A (2000) Auxetic materials: functional materials and structures from lateral thinking! *Adv Mater* 12(9):617–628
32. Lakes R (1987) Foam structures with a negative Poisson's ratio. *Science* 235(4792):1038–1040
33. Critchley R, Corni I, Wharton JA et al (2013) A review of the manufacture, mechanical properties and potential applications of auxetic foams. *Phys Status Solidi B* 250(10):1963–1982
34. Chan N, Evans KE (1999) The mechanical properties of conventional and auxetic foams. Part I: compression and tension. *J Cell Plast* 35(2):130–165
35. Scarpa F, Pastorino P, Garelli A et al (2005) Auxetic compliant flexible PU foams: static and dynamic properties. *Phys Status Solidi B* 242(3):681–694
36. Grima JN, Attard D, Gatt R et al (2009) A novel process for the manufacture of auxetic foams and for their re-conversion to conventional form. *Adv Eng Mater* 11(7):533–535
37. Lisiecki J, Błażejewicz T, Kłysz S et al (2013) Tests of polyurethane foams with negative Poisson's ratio. *Phys Status Solidi B* 250(10):1988–1995
38. Friis EA, Lakes RS, Park JB (1988) Negative Poisson's ratio polymeric and metallic foams. *J Mater Sci* 23(12):4406–4414
39. Alderson A et al (2005) The effects of processing on the topology and mechanical properties of negative Poisson's ratio foams. In: *Proceedings of ASME International Mechanical Engineering Congress and Exposition (Aerospace Division)*, Orlando, Florida, November 2005, vol 70AD, p 503
40. Lowe A, Lakes RS (2000) Negative Poisson's ratio foam as seat cushion material. *Cell Polym* 19(3):157–168
41. Lisiecki J, Kłysz S, Błażejewicz T et al (2014) Tomographic examination of auxetic polyurethane foam structures. *Phys Status Solidi B* 251(2):314–320
42. Chan N, Evans KE (1997) Fabrication methods for auxetic foams. *J Mater Sci* 32(22): 5945–5953

43. Pastorino P, Scarpa FL, Patsias S et al (2007) Strain rate dependence of stiffness and Poisson's ratio of auxetic open cell PU foams. *Phys Status Solidi B* 244(3):955–965
44. Bezazi A, Scarpa F (2007) Mechanical behaviour of conventional and negative Poisson's ratio thermoplastic polyurethane foams under compressive cyclic loading. *Int J Fatigue* 29(5): 922–930

Open Access This chapter is distributed under the terms of the Creative Commons Attribution-Noncommercial 2.5 License (<http://creativecommons.org/licenses/by-nc/2.5/>) which permits any noncommercial use, distribution, and reproduction in any medium, provided the original author(s) and source are credited.

The images or other third party material in this chapter are included in the work's Creative Commons license, unless indicated otherwise in the credit line; if such material is not included in the work's Creative Commons license and the respective action is not permitted by statutory regulation, users will need to obtain permission from the license holder to duplicate, adapt or reproduce the material.

